HAL open science

Integrated untargeted metabolomics and bioactivity studies as new insights into the chemotaxonomy of Hura crepitans specimens from Peru and Sub-Saharan Africa

Elise Crossay, Valérie Cristofoli, Pedro Vásquez-Ocmín, Gabriel Vargas-Arana, Hospice Dassou, Arthur-Joel Semedo, Mamoudou Alao, Guillaume Marti, Nicolas Fabre

To cite this version:

Elise Crossay, Valérie Cristofoli, Pedro Vásquez-Ocmín, Gabriel Vargas-Arana, Hospice Dassou, et al.. Integrated untargeted metabolomics and bioactivity studies as new insights into the chemotaxonomy of Hura crepitans specimens from Peru and Sub-Saharan Africa. Journal of Pharmaceutical and Biomedical Analysis, 2024, 255, pp.116583. ⟨10.1016/j.jpba.2024.116583⟩. ⟨hal-04909510⟩

HAL Id: hal-04909510

https://hal.science/hal-04909510v1

Submitted on 24 Jan 2025

HAL is a multi-disciplinary open access archive for the deposit and dissemination of scientific research documents, whether they are published or not. The documents may come from teaching and research institutions in France or abroad, or from public or private research centers.

L'archive ouverte pluridisciplinaire **HAL**, est destinée au dépôt et à la diffusion de documents scientifiques de niveau recherche, publiés ou non, émanant des établissements d'enseignement et de recherche français ou étrangers, des laboratoires publics ou privés.

Distributed under a Creative Commons CC BY 4.0 - Attribution - International License

Journal of Pharmaceutical and Biomedical Analysis 255 (2025) 116583

Contents lists available at ScienceDirect

Journal of Pharmaceutical and Biomedical Analysis

journal homepage: www.journals.elsevier.com/journal-of-pharmaceutical-and-biomedical-analysis

Integrated untargeted metabolomics and bioactivity studies as new insights into the chemotaxonomy of *Hura crepitans* specimens from Peru and Sub-Saharan Africa

Elise Crossay [a], Valérie Cristofoli [a], Pedro Vásquez-Ocmín [a], Gabriel Vargas-Arana [b], Hospice Dassou [c], Arthur-Joel Semedo [d], Mamoudou Alao [e], Guillaume Marti [f,g,1], Nicolas Fabre [a,*,1]

[a] UMR 152 PharmaDev, Université de Toulouse, IRD, UPS, France
[b] Instituto de Investigaciones de la Amazonía Peruana (IIAP), Iquitos, Peru
[c] Université d'Abomey-Calavi, Benin
[d] Société 'Terre Victorieuse', Togo
[e] Hôpital Nord Franche-Comté, France
[f] Laboratoire de Recherche en Sciences Végétales, Metatoul-AgromiX Platform, Université de Toulouse, CNRS, INP, 24 Chemin de Borde Rouge, Auzeville, Auzeville-Tolosane 31320, France
[g] MetaboHUB-MetaToul, National Infrastructure of Metabolomics and Fluxomics, Toulouse, France

ARTICLE INFO

Keywords:
Hura crepitans
Untargeted metabolomic studies
Daphnane
Cytotoxicity

ABSTRACT

Hura crepitans (Euphorbiaceae), is widespread in the Amazon rainforest and on plantations in sub-Saharan Africa. This tree produces an irritating milky latex rich in secondary metabolites, notably daphnane-type diterpenes and cerebrosides. Previous studies have shown that huratoxin, the main daphnane in the latex, significantly and selectively inhibited the growth of colorectal cancer cells through a unique mechanism involving the activation of PKCζ. One major challenge in isolating active molecules from natural products is the accessibility of the resource. This study explores the phytochemical composition and cytotoxic activities of latexes collected in Peru, Benin, and Togo using UHPLC-MS and metabolomics tools to identify a renewable source of bioactive compounds. Significant inter- and intra-continental differences in chemical composition have been highlighted, with daphnanes being concentrated in the Peruvian samples. Extracts form latexes collected in Peru showed cytostatic activity on Caco-2 cells, correlated with the presence of daphnanes, while some African samples exhibited cytotoxic activity on Jurkat and Hela cancer cell lines, leading to the identification of potential other new bioactive compounds such as elasterol and cerebrosides.

Objective: To compare the composition of different *Hura crepitans* latex samples and determine their cytotoxic activity in order to identify new bioactive compounds

Conclusions: Inter- and intra-continental variations in the phytochemical composition of latex were observed, leading to significant cytotoxic activities on different cell lines. Daphnanes were identified as responsible for the activity on Caco-2 cells, while elasterol and cerebrosides were putatively associated with the activity on Hela cells.

1. Introduction

Hura crepitans L. is a member of the Euphorbiaceae family, widespread in South America, Africa and Asia [1–3]. This thorn-covered tree can reach heights of 35–60 m, depending on environmental conditions. Its leaves can grow up to 30 cm in length and it is distinguished by red petal-less flowers and dehiscent capsule-shaped fruits composed of eleven to fourteen carpels [1]. *H. crepitans* also produces an irritant latex containing numerous secondary metabolites [1–3]. Our previous phytochemical studies focused on South America species, particularly

* Correspondence to: UMR 152 PharmaDev, Université Paul Sabatier, Faculté de Pharmacie, 35 Chemin Des Maraichers, CEDEX 3, Toulouse 31062, France.
E-mail address: nicolas.fabre@univ-tlse3.fr (N. Fabre).

[1] These authors contributed equally to the work

https://doi.org/10.1016/j.jpba.2024.116583
Received 30 September 2024; Received in revised form 19 November 2024; Accepted 24 November 2024
Available online 4 December 2024
0731-7085/© 2024 The Author(s). Published by Elsevier B.V. This is an open access article under the CC BY license (http://creativecommons.org/licenses/by/4.0/).

on Peruvian latex extracts, which revealed two main families of compounds: daphnane diterpenes (mono- and diesterified) and cerebrosides [4] (Fig. 1).

Monoesterified daphnanes, especially huratoxin, the main daphnane diterpene in latex, exhibited promising cytostatic activity against colorectal cancer cells including Caco-2 cell line and colorectal cancer cells cultured as colonoid, with high selectivity [5,6]. Colorectal cancer (CRC) ranks as the third most common cancer worldwide and the second most deadly [7,8]. At the metastatic stage, the 5-years survival rate is only about 5–15 % [9]. The development of new therapies for colorectal cancer is a global health issue. In this context, *H. crepitans* could be a promising source of new bioactive molecules, particularly daphnane diterpenes contained in its latex. However, one of the main limitations concerning the isolation of active molecules from natural products is access to the resource. As *H. crepitans* is used as a pepper tree stake in Africa, notably in Benin and Togo, collecting latex on plantations becomes more feasible compared to the challenges posed by the Amazonian rainforest. In addition, plant adaptation to different environmental conditions, such as climate or soil composition, could lead to the development of a reservoir of chemical diversity.

However, to our knowledge, there are no recent studies on the phytochemical composition of *H. crepitans* latex collected in Africa because the literature primarily focuses on other parts of the plant such as leaves, seeds and stem barks [1,10,11]. It is therefore interesting to investigate the phytochemical composition of African latex and compare it with that of Peruvian latex using a metabolomic approach.

Metabolomic allows for the identification and quantification of numerous components within complex mixture, whereby all of the acquired data can be leveraged to compare phytochemical composition between extracts [12]. However, the ability of metabolomics to encompass the full complexity of phytochemical blends greatly depends on the method used to capture the data. For instance, it has been shown that separative methods provide more accurate statistical models and higher identification rates compared to direct spectroscopic fingerprinting [13].

Following on from our previous works on Peruvian *H. crepitans* daphnanes [4–6], and in order to identify renewable sources for obtaining monoesterified daphnanes and possibly detecting new ones, the present work focused on the chemical analysis and cytotoxicity on cancerous cell lines of various *H. crepitans* latex samples collected in South America (Peru) and Africa (Togo, Benin). A metabolomic approach was then conducted to highlight the main differences between the samples. Multivariate statistical analyses were used to emphasize the most discriminative spectrometric signals of each class. First, PCA provided an unsupervised overview of the dataset. Then, orthogonal PLS-DA, known for revealing group differences while filtering noise, was applied. Finally, the Shared Unit Structure plot (SUS-plot) exhibited main biomarkers for each group. Additionally, molecular networking was constructed to improve compound annotation using their MSMS spectra.

2. Material and method

2.1. Plant material

Peruvian latex samples from six *Hura crepitans* specimens were collected in December 2021 in the *Cocha Vainilla* area, (Coordinates UTM 640726, 9458471; elevation 110 m.a.s.l; zone 18, District of Jenaro Herrera, Province of Requena, Region of Loreto). Botanical identification was based on specimens from the Arboretum of the Jenaro Herrera Research Center "José López Parodi" and was performed by botanist Nallarett Davila.

Latexes of *H. crepitans* from Africa were collected in southern Benin (12 specimens in 3 locations: Ouidah (6°21'33.196 ''N / 2°5'25.022''), Ahita (6°42'06''N / 2°37'30''E) Ofia (7°21'38.505''N / 2°39'3.02''E)) and in Dafo, Togo (5 specimens in the same location).The collected specimens were identified as *Hura crepitans* L. by Professor Haunnankpon Yedomohnan, conservator of the National Herbarium of Benin in Africa.

2.2. Extraction of the latex of H. crepitans

Notches were made in the trunks of several *H. crepitans* to collect the latex. The lyophilizated latex (1 g per specimen) was then extracted with 10 mL of 96 % EtOH during 2 h, under reflux with stirring. After two successive paper filtrations (particle retention from 5 to 13 μm), 23 extracts were obtained: B1 to B6, A1 and A2 and O1 to O4 (latexes from Benin); D1 to D5 (Togo) and P1 to P6 (Peru). Extractions were performed in triplicate, followed by an evaporation step under vacuum.

2.3. Sample preparation

Dry samples were solubilized in absolute EtOH at a concentration of 10 μg/mL for extracts and 1 μg/mL for huratoxin. Ten μL of each sample were pooled to form QC.

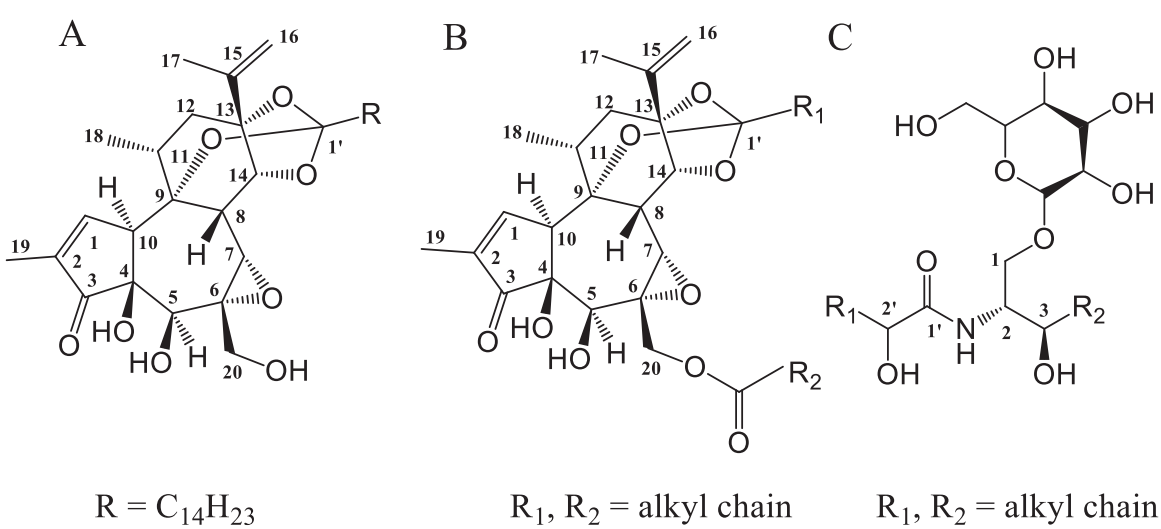

Fig. 1. General structure of huratoxin (A), diesterified daphnanes (B) and cerebrosides (C).

2.4. UHPLC-HRMS profiling

UHPLC/DAD/HRMS analyzes were performed using an UHPLC Ultimate 3000 system (Dionex) equipped with LTQ-Orbitrap XL mass spectrometer (Thermo Fisher Scientific), a Diode Array Detector (Dionex) and a Phenomenex Luna Omega C18 UPLC 100 Å column (2,1 × 150 mm, 1,6 μm). Ionization was performed using an atmospheric pressure chemical ionization source (APCI) functioning in the positive ionization mode at 15,000 resolving power (full width at half maximum (FWHM) at 400 *m/z*). The capillary temperature was 275°C and spray voltage was fixed at 5 kV. The mass scanning range was *m/z* 100–2000 Da. Each full MS scan was followed by data dependent MS/MS with dynamic exclusion (repeat count 3) using stepped collision-induced dissociation (CID) (35 normalized collision energy, isolation width 1 Da, activation Q 0.025). Chromeleon Xpress 6.8 (Dionex) and Xcalibur 3.0 (Thermo Fischer Scientific) softwares were used for data acquisition and analysis. Mobile phases were deionized water (A) and acetonitrile (B) acidified with 0.1 % formic acid. Gradient conditions were: 0 min, 10 % A; 2 min, 10 % A; 22 min, 0 % A; 36 min, 0 % A; 37.5 min, 10 %A and 40 min 10 % A. The flow rate was 0.4 mL/min, column temperature 40°C and 16 μL of all extracts at 0.5 mg/mL were injected.

2.4.1. Data processing

The UHPLC-HRMS raw data were processed with MS-DIAL version 5.1 [14] for mass signal extraction between 0 and 2000 Da, from 0.53 to 40 min. MS1 and MS2 tolerance were set to 0.01 and 0.025 Da in centroid mode respectively and the detection threshold was set to 1×10^6 for MS1 and 10 for MS2. Peaks were aligned on a quality control (QC) reference file with a retention time tolerance of 0.2 minutes and a mass tolerance of 0.015. Finally, MS-CleanR [15] peaks filtering were set with these parameters: minimum blank ratio 0.8, maximum RSD 40, RMD 50–3500 and ghost peaks were deleted.

2.4.2. Identification of significant features

Molecular formula of significant features were calculated with MS-FINDER 3.60 [16]. Various parameters were used in order to reduce the number of potential candidates, such as the element selection exclusively including C, H, O, N; mass tolerance fixed to 15 ppm for MS1 and 50 ppm for MS2, the isotopic ratio tolerance set to 20 %. The annotation was conducted with three levels of confidence [17]: manual annotation with inspection of MS-MS spectrum and in-house database matching (level 2), and comparison with general databases (level 3). For natural product databases, selections were made from the Universal Natural Products Database (UNPD), Natural Products Atlas (NPA), COCONUT, North African Natural Products Database (NANPDB), KNApSAcK, PlantCyc, and PubChem. The results were presented as a list of compounds sorted according to the score value of the match. This value encompassed uncertainty on accurate mass, the isotopic pattern score and the experimental MS/MS fragmentation mirrored to *in silico* matches. Additionally, manual inspection of MS2 fragmentation pattern according to a previously published paper [4], allowed the dereplication of daphnanes derivatives.

2.4.3. Statistical analysis

For each feature, the mean peak height of the triplicates of extraction was used. Then, comma-separated value files exported from MS-DIAL were imported into SIMCA-P + (version 14.1, Umerics, Umea, Sweden) after adducts and neutral losses were manually removed (see StatTable.csv file on Supplementary data). For all data, Pareto scale was used. An unsupervised overview of chemical profiles was obtained using Principal Component Analysis (PCA). A discriminative model was set-up to separate extract origin from Africa and Peru. The SUS-plot and VIP coefficient from Orthogonal Projection to Latent Structure-discriminant Analysis (OPLS-DA) model, were used to highlight most discriminant compounds. A PLS regression analysis was done with cytostatic activity (% of growth inhibition of Caco-2 cells) values as Y input and coefficient scores were used to rank variables statistically correlated to the cytostatic activity.

Univariate analyses were carried out in Excel using the correlation coefficient function. This approach allowed for the assignment of a coefficient to each feature, representing its correlation with the percentage of growth inhibition on Jurkat and Hela cells.

2.4.4. Mass spectral similarity network

Text files exported from MS-DIAL were imported into Cytoscape 3.10.1 [18]. Files were exported with the Bonanza score method, mass tolerance was set at 0.2 Da, and similarly cut off at 60 %.

Adducts and neutral losses were manually removed. Feature with similarity score between 0.6 and 1 were selected to build the mass spectral similarity network. An attribute file containing all processed information, in particular *m/z* values, PLSDA VIP coefficients and chemical classes of identified features were imported to enhance network visualization (see Nodes.csv and EdgeAll.csv files on Supplementary data).

2.5. Biological assay

2.5.1. Cell cultures

The human colon adenocarcinoma cell line Caco- 2 (HTB-37TM), the human cervical carcinoma cell line Hela and the human lymphocyte T from leukemia cell line Jurkat were purchased from the American Type Culture Collection (ATCC). Caco-2 cells were cultured in DMEM medium with 4.5 g/L of glucose, 1 % GlutaMAX and 1 % pyruvate (GIBCO, 31966) supplemented with 10 % FBS (GIBCO), 1 % non-essential amino acids (GIBCO) and 1 % penicillin and streptomycin mixture (P/S, GIBCO). Hela cells were cultured in MEM medium (biowest), while Jurkat cells were cultured in RPMI medium (Sigma-Aldrich), both supplemented with 10 % FBS and 1 % P/S. All cells were cultured at 37 ∘C in 5 % CO2 incubator and media were changed every 48 h and passages were done at 90 % of confluence.

2.5.2. Cytotoxicity tests

Forty-eight hours before cytotoxicity test, 10,000 (Caco-2 and Hela assays) cells/well were seeded in 96-wells plates (Thermo Fisher Scientific), while Jurkat cells were seeded at 20,000 cells/wells on the same day as treatment with extracts. All extracts and huratoxin were dissolved in dimethyl sulfoxide (DMSO, Thermo Fisher Scientific) at 100 mg/mL and 10 mg/mL, respectively, followed by successive dilutions with medium to obtain final concentration (10 μg/mL for extracts and 1 μg/mL for huratoxin). At 48 h after cells seeding, extracts were added in triplicates with DMSO as a negative control (maximum concentration 0.01 %) and doxorubicin as positive control (1 μg/mL). After 48 h, MTS (Cell line assay, CellTiter 96 AQueous One Solution Cell Proliferation Assay, Promega) was added on each well and cytotoxicity tests were performed according to the manufacturer's instructions. Then, cell viability was measured by colorimetry at 490 nm (BioTek Eon™ High Performance Microplate Spectrophotometer). The growth inhibition percentages ± SEM of doxorubicin (n = 2–3) were 57 % ± 0.7, 39 % ± 4.5 and 17 % ± 4.0 for Jurkat, Caco-2 and HeLa cell lines, respectively.

2.5.3. Statistical analysis

Statistical analyzes were performed using GraphPad Prism 8. Student's *t*-test was used for experiments analysis. P values < 0.05 were considered to be significant.

3. Results and discussion

3.1. Multivariate analysis of the different latex extracts

UHPLC-HRMS analysis of all 70 extracts (18 from Peru, 51 from

Africa and 1 QC sample) yielded 741 features, including MSMS, in positive ion mode, after data processing with MS-Dial and MS-CleanR. Subsequently, adducts and neutral losses were manually removed leading to 540 features. Firstly, principal component analysis (PCA) was conducted to provide an unsupervised overview of the LC-MS fingerprints, leading to the identification of three distinct groups: Peruvian samples in red, Beninese samples from Ahita and Ofia in blue, and Togolese and Beninese samples from Ouidah in green (Fig. 2A). OPLS-DA was then achieved to cluster the samples according to these three groups with good model prediction (R2Y = 0.965, Q2 = 0.924, CV-

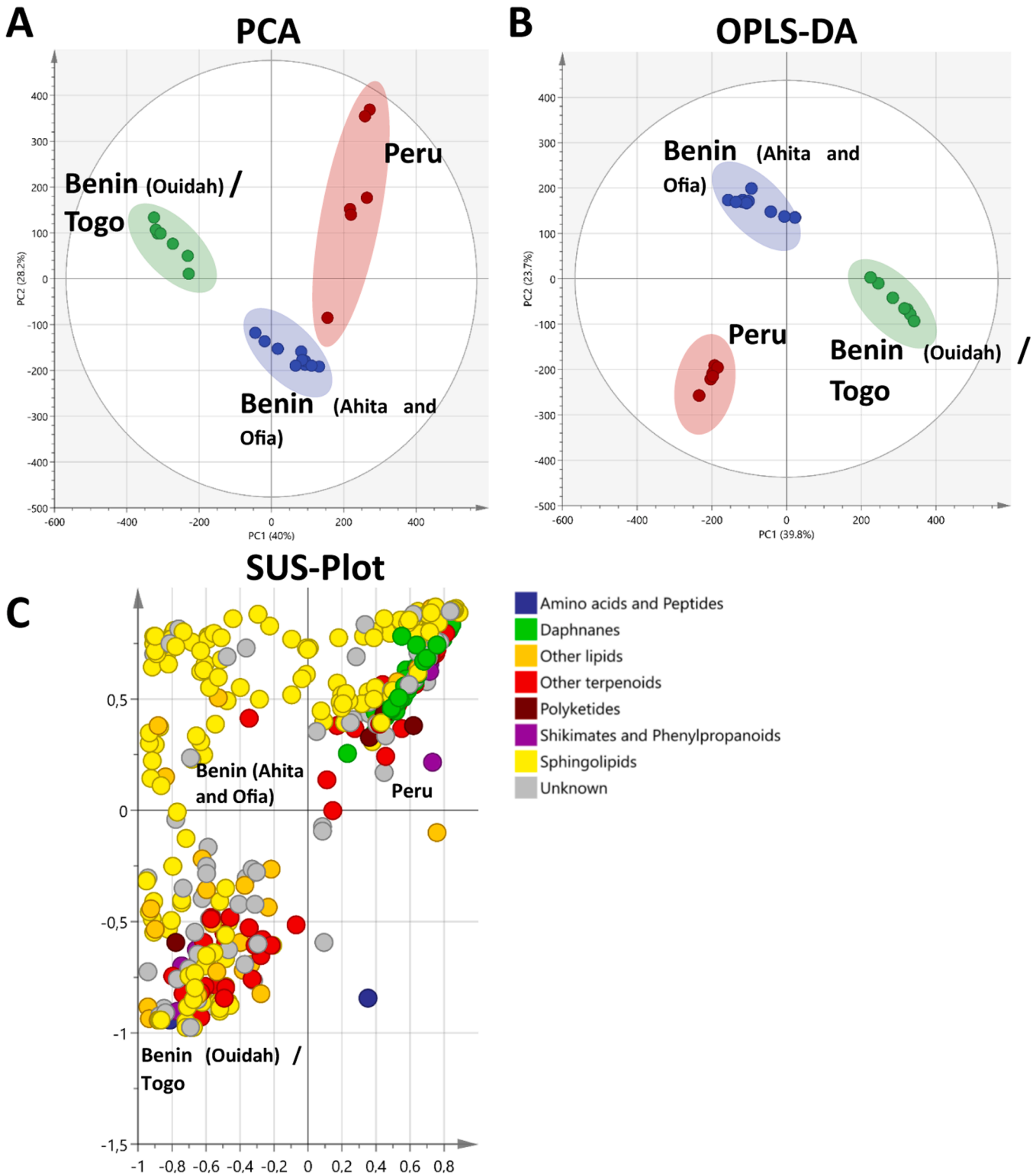

Fig. 2. Comparison of phytochemical composition of *H. crepitans* latex extracts. PCA (A) and OPLSDA (B) of the APCI-POS ionization dataset are shown. Peruvian samples are in red, African samples from Ahita and Ofia (Benin) are in blue, and African samples collected in Togo and Ouidah (Benin) are in green. The SUS-plot of the OPLS-DA analysis (C) compares the Peruvian samples with African samples from Benin (Ouidah) and Togo (bottom left corner), and with African samples from Benin (Ahita and Ofia) (top left corner).

Anova < 0.001) (Fig. 2B). OPLS-DA analysis revealed a separation between African and Peruvian samples, indicating significant differences in the composition of latexes from the two sites. Considering that the southern regions of Benin and Togo and northern regions of Peru (collection sites) share a similar equatorial climate, the observed inter-continental differences could be attributed to another environmental factor. In particular, biotic stress such as exposure to insects, herbivores, bacteria, and fungi can influence their phytochemical composition as already established by Salomé-Abarca and colleagues for latex of *Euphorbia* species [19]. Furthermore, abiotic stresses such as salinity, UV radiation, and heavy metals can also modify the plant metabolome [20].

In addition, intra-continental differences also emerged (Figs. 2A and 2B). It can be observed that the African extracts were further separated into two groups: samples collected in Benin (Ouidah) and Togo, trees

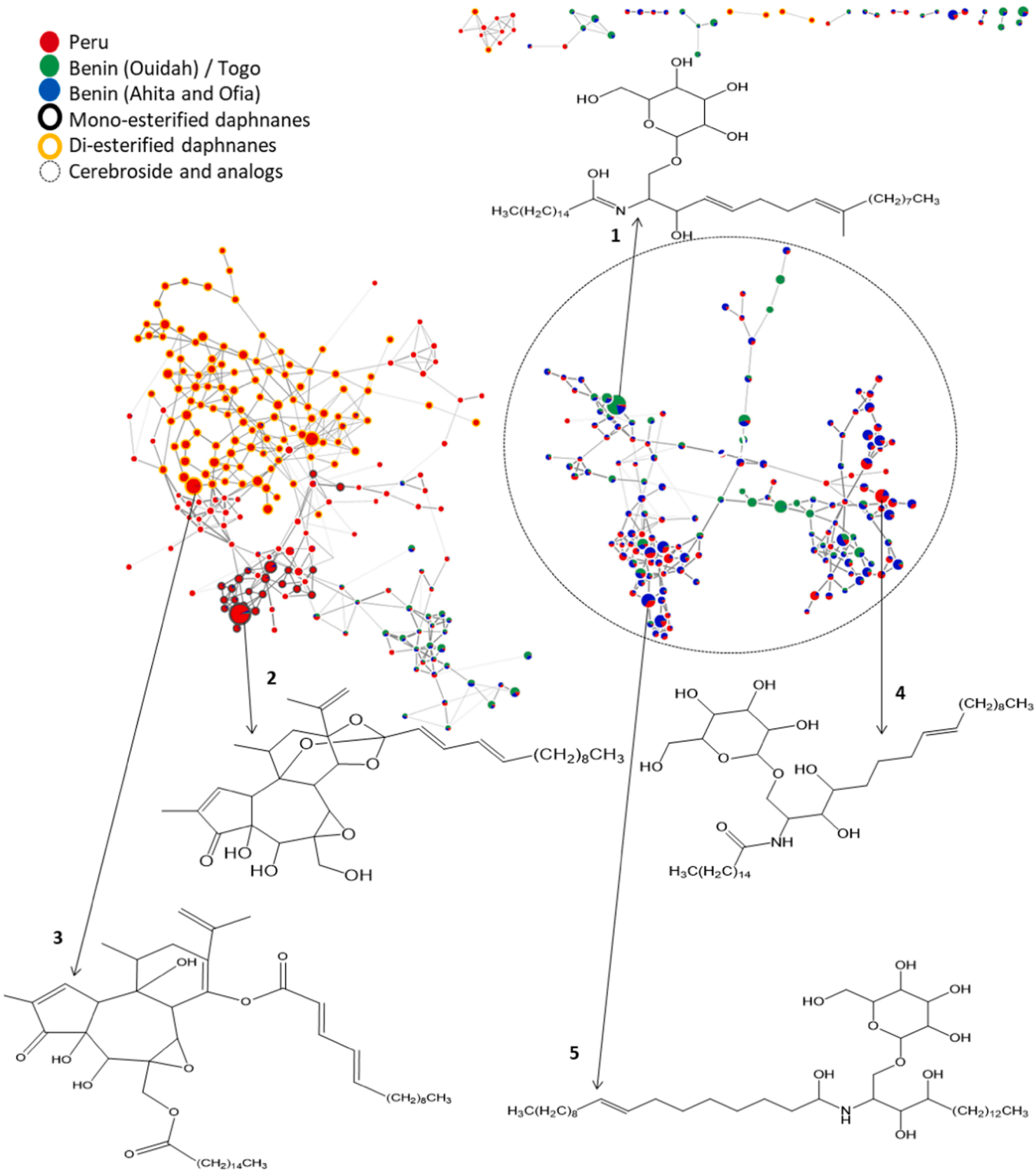

Fig. 3. Mass spectral similarity network of *H. crepitans* latex extracts from Peru and Africa. Structures of top five compounds, ranked by the VIP score of the OPLSDA regression analysis were shown.

aged from 4 to 6 years and extracts collected exclusively in Benin (Ahita and Ofia), trees aged from 20 to 80 years old. Interestingly, one Peruvian sample appears to be more closely related to the African extracts than to the other Peruvian samples. Thus, for the same continental location, developmental stage of the plant could be implicated in its chemotype, as previously mentioned by Rodziewicz et al. [20].

After OPLS-DA, a Shared Unique Structure (SUS)-plot was generated using OPLS-DA regression analysis (Peru/Benin (Ahita and Ofia) R2Y = 0.998, Q2 = 0.974, CV-Anova < 0.001; Peru/ Benin (Ouidah) and Togo R2Y = 0.993, Q2 = 0.974, CV-Anova < 0.001) (Fig. 2B). This supervised method enabled to classify the most discriminating features between different groups (Fig. 2C). Features were colored according to their chemical class. Daphnane diterpenes were manually annotated (level 2) due to their characteristic MSMS fragments, observed in positive ionization mode, at *m/z* 361, 325, 307, 297, 279, 253 for an huratoxigenin core (Fig. 1A) and at *m/z* 311, 293, 283, 265 for a 5-deoxy-6,7-deepoxydidehydro-huratoxigenin skeleton (Figs. 1 and 2 in SI), as previously described by our group [4]. Other compounds were annotated using *in silico* natural product databases (level 3) in MS-FINDER. For each feature, the results provided several candidates ranked according to their similarity scores, which were determined by comparison with experimental MSMS fragments and *in silico* spectra of the candidates. As shown in Fig. 2C, sphingolipids (colored in yellow) are abundant in each group, whereas daphnanes (in green) are concentrated in Peruvian extracts. Furthermore, latexes collected at Ahita and Ofia (Benin) are almost exclusively composed of sphingolipids and other lipids (orange-labeled), while latexes collected in Togo and Ouidah (Benin) contain other terpenoids besides daphnanes, mostly sesqui- and tri-terpenoids (red-labeled). Terpenoids may be linked to the latex's defense role against biotic stress, explaining their accumulation in this part of the plant. Moreover Salome-Abarca *et al.* concluded that the latex composition of *Euphorbia* species collected from different regions of Slovenia, particularly the amount of triterpenes, showed a low degree of variation with respect to geographical location and environmental stresses [19]. It is therefore surprising that the Beninese group contains no terpenoid compounds. A comparative analysis of the genomes of the different trees would be valuable to better understand the differences in metabolite production.

3.2. Mass spectral similarity network

For better visualization of the phytochemical composition of the extracts, mass spectral similarity network was constructed (Fig. 3). The latter highlighted two major clusters: daphnane analogs (on the left) and cerebroside derivatives (on the right side). Mono- and diesterified daphanes were manually annotated and surrounded in black and yellow, respectively, while cerebrosides cluster was outlined with a dotted line. VIP coefficients from OPLS-DA analysis were used to adjust node size, and the structures of the top five compounds were shown. Additionally, a pie chart was generated for each node, representing the abundance of each compound in African (green or blue) or Peruvian (red) latex. Finally, edges width was set based on the MSMS similarity score.

The mass spectral similarity network confirms that daphnanes and cerebrosides are the main components of *H. crepitans* latex [4]. Interestingly, daphnane diterpenes are mainly present in Peruvian extracts (in red) and nearly absent from African ones (shown in green and blue), whereas cerebrosides appear to be distributed in both locations (Fig. 3). A decrease in the production of terpenoid compounds, particularly carotenoids, in response to climatic conditions was already observed in drought-stressed cotton [20]. More recently, Zheng *et al.* demonstrated the influence of genotype on metabolite production in two *Euphorbia* species, noting that two genes involved in diterpenoid biosynthesis were sensitive to adaptive mutations. Thus, the accumulation of different metabolites can reflect a plant's adaptation to varying environmental conditions [21].

The daphnane cluster indicates that di-esterified daphnanes (surrounded in yellow) are more abundant than mono-esterified derivatives (surrounded in black). Previous study on *H. crepitans* latex extracts collected in the same location in Peru, showed the opposite proportion of mono- and di-esterified daphnanes [4], confirming that phytochemical composition not only depends on geographic condition but can also be influenced by other biotic and/or abiotic parameters. It is worth noting that three collections were conducted for the Peruvian samples: February 2017, September 2019, and December 2021 (for the present study). Di-esterified daphnanes from *H. crepitans* are not extensively described in the literature, which is promising for the discovery of new natural products. However, cytostatic activity on Caco-2 cells appears to be driven by mono-esterified derivatives [5].

Top five discriminating features between groups are huratoxin, a di-esterified daphnane and three cerebrosides, respectively compounds **2**, **3**, **1**, **4** and **5** (drawn in Fig. 3). For the unknown di-esterified compound, dereplication was performed based on its MSMS spectrum obtained from the $[M+H]^+$ ion at *m/z* 823.57397 and Rt 26.26 min (no. 3 in Fig. 3). The dereplication reasoning set out below was applied for the other annotated di-esterified daphnanes. As depicted in Fig. 4, the characteristic fragments of a huratoxigenin core are present. Additionally, it can be observed three successive dehydrations from the molecular ion at *m/z* 805, 787 and 769, thus indicating a compound with two monoesterified alkyl chains. Indeed, an orthoesterified chain allows only two dehydrations from molecular ion since one hydroxyl group of the diterpene core is engaged in the link with alkyl side chain (see Fig. 1). The neutral loss of 224 uma ($C_{14}H_{24}O_2$), resulting in the ion at *m/z* 599, indicates the loss of the C14-doubly unsaturated alkyl chain. The most probable localization for this chain is the C-14 carbon of the huratoxigenin since all daphnanes previously isolated from *H. crepitans* are (ortho)esterified in C-14 [5,6]. As expected, three dehydrations occur from the $[M+H-C_{14}H_{24}O_2]^+$ ion at *m/z* 599 leading to fragments at *m/z* 581, 563 and 545. The structure of the second esterified chain was easily deduced from the difference 599 minus 361 implying a neutral loss of 238 u, corresponding to a saturated 16-carbon alkyl chain. The most likely location of this chain is the methylene alcohol at C-20 as previously described by Adolf and Hecker in 1984 [22]. Thus, this compound was named 20-hexadecanoyl-huratoxin(monoester).

3.3. Correlation of the cytotoxic activity and the phytochemical composition of the H. crepitans latex extracts from Peru and Africa

3.3.1. Cytotoxicity against Caco-2 cells

Our previous studies have demonstrated that monoesterified daphnanes of *H. crepitans*, especially huratoxin, isolated from a latex collected in Peru, exhibit notable selective cytostatic activity on the colorectal cancer cell line Caco-2, as well as on primary cells cultured as organoids [5,6]. Additionally, an original mechanism of action involving PKCζ was established for this compound [6]. In this context, Caco-2 cells were used as cellular model to compare the biological activities of our extracts.

The Fig. 5A depicts the cytostatic activity of Peruvian (left) and African (right) latex extracts normalized to the effect of DMSO (control). As illustrated, huratoxin exhibits the better antiproliferative effect (20 % of growth inhibition at a concentration of 1 μg/mL) on Caco-2 cells, when compared to the different extracts (at a concentration of 10 μg/mL). Extracts collected in Peru showed varying activity on Caco-2 cells, so each Peruvian sample was represented individually, while African extracts were grouped according to their geographical collection sites. As pictured in Fig. 5A, Peruvian extracts, except for tree no. 5, showed significative cytostatic activity with 10–15 % of growth inhibition on Caco-2 cells. Additionally, the latex extract obtained from tree no. 1 exhibited a more potent cytostatic activity than trees no. 3, 4 and 6. Concerning African samples, none of the extracts showed a significative cytostatic activity. This can be explained by the fact that monoesterified daphnanes, which were proved to be responsible for the cytostatic activity on Caco-2 cells [5], are concentrated in Peruvian extracts and

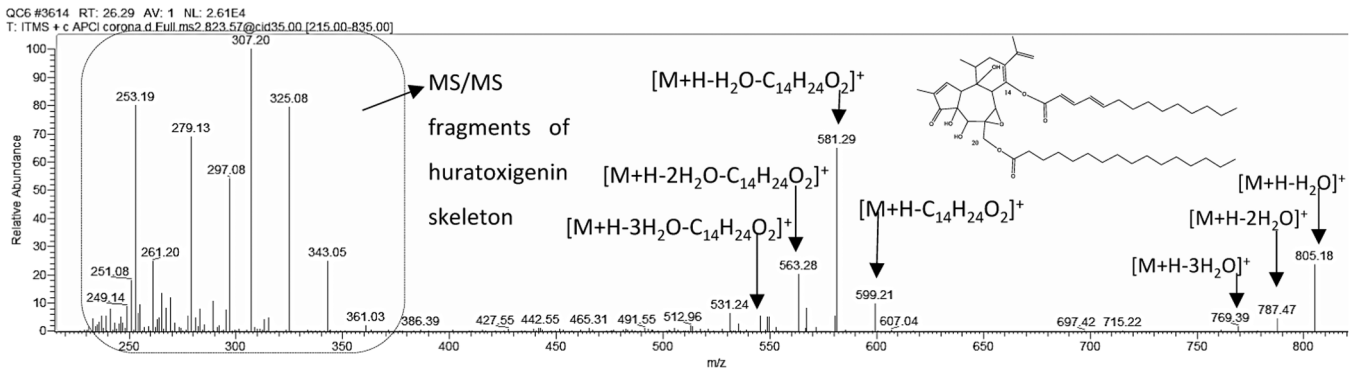

Fig. 4. MSMS spectra of 20-hexadecanoyl-huratoxin(monoester) (m/z 823.57, RT = 26.26 min).

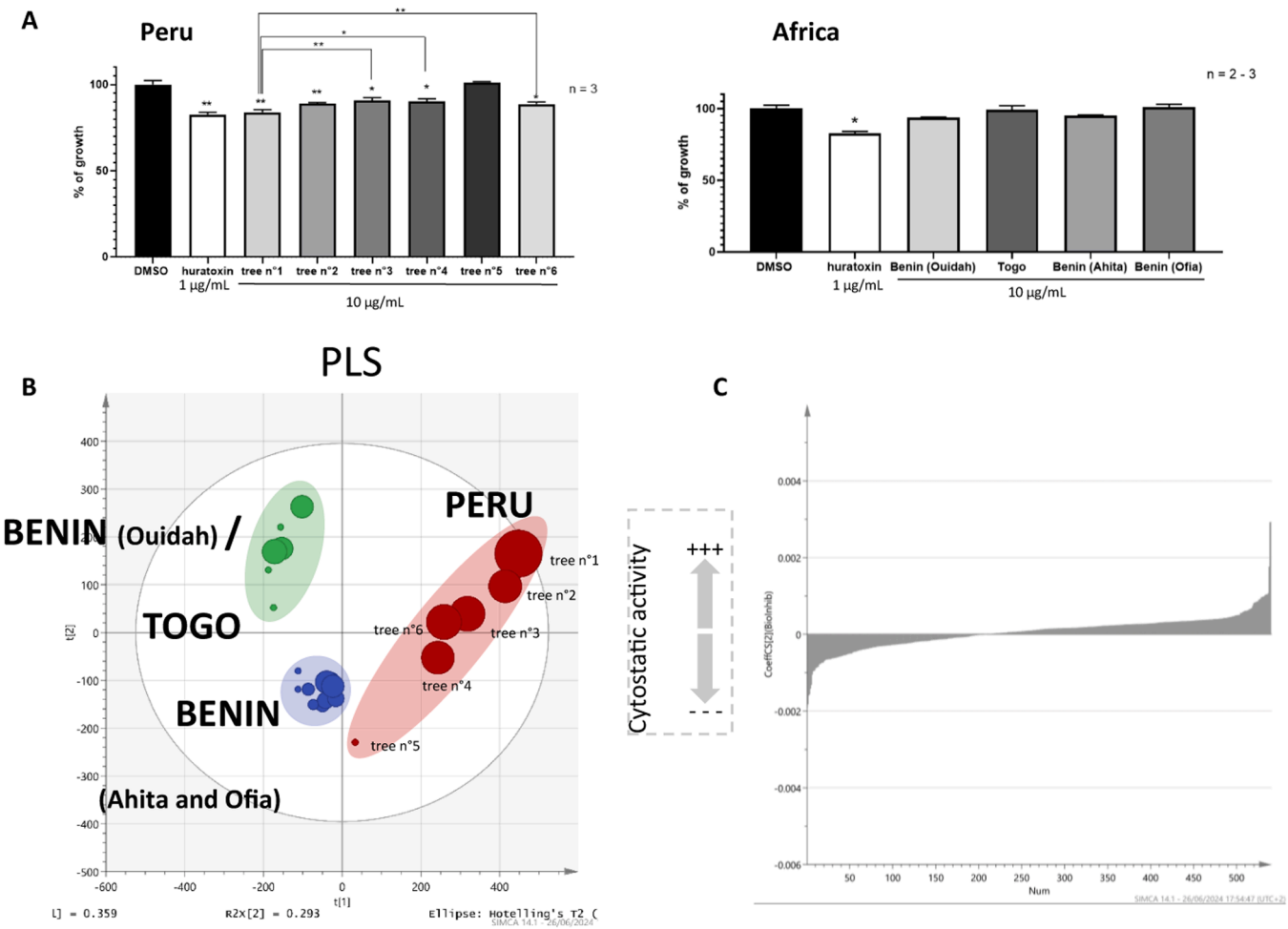

Fig. 5. Correlation of the cytostatic activity on Caco-2 cells and the phytochemical composition of the *H. crepitans* latex extracts from Peru and Africa. A) Activity of Peruvian (left) or African (right) extracts on Caco-2 cells. Cells were incubated with extracts (10 µg/mL) or huratoxin (1 µg/mL) as a positive control during 48 h then cell viability was measured by colorimetry and compared to control (DMSO). Mean ± SEM, *t*-test from triplicates of 2–3 independent experiments. * $p < 0.05$, ** $p < 0.01$. B) PLS score plot of APCI-POS ionization dataset, with cytostatic activity as Y input. The node size was correlated with the cytostatic activity of the sample on Caco-2 cells. C) Coefficient plot obtained by PLS regression.

rarely found in African samples (Fig. 3). Interestingly, the Peruvian latex extract obtained from tree no. 5 showed no cytostatic activity. As depicted in the PCA (Fig. 2A), the extract from Peruvian tree no. 5 is distant from the other Peruvian samples, suggesting significant differences in chemical composition, thus explaining this absence of cytostatic activity against Caco-2 cells.

In order to detect compounds responsible for these differences, PLS regression analysis was applied to classify samples according to their cytostatic activity (percentage of Caco-2 cells growth inhibition as Y input, R2Y = 0.75, Q2 = 0.553, CV-Anova = 0.004), and features were ranked based on their regression coefficient values (Figs. 5B, 5C): positive coefficients were correlated with potential cytostatic activity, while negative ones were associated with less-active compounds. From the list containing the first hits (Table 1), an annotation based on their MSMS spectra is proposed. As expected, huratoxin, a known active monoesterified daphnane, ranks first followed by two diesterifed daphnanes.

Table 1
Top three compounds correlated with the cytostatic activity on Caco-2 cells.

PLS Rank	$[M+H]^+$	RT (min)	MF	PLS coefficients	Identification/ *Annotation*
1	585.34381	3.64	$C_{34}H_{48}O_8$	0.002923415	Monoesterified daphnane huratoxin
2	823.57397	26.26	$C_{50}H_{78}O_9$	0.00292309	Diesterified daphnane *20-hexadecanoyl-huratoxin (monoester)*
3	847.57233	23.24	$C_{52}H_{78}O_9$	0.001767752	Diesterified daphnane *20-octadec-dien-oyl-huratoxine (monoester)*

To further explain the differences in activity among the six Peruvian samples, normalized peak areas of the top three compounds correlated with potential cytostatic activity on Caco-2 cells were graphically represented (Fig. 6). As depicted in Fig. 6, the top three features correlated with cytostatic activity are absent in the latex extract of Peruvian tree no. 5, which explains its lack of activity. This observation underlines the fact that specimens located in the same area can have very different chemotypes. Moreover, huratoxin is more abundant in the latex extract of trees no. 2 and 4 and almost absent in trees no. 3 and 6 (Fig. 6). However, there is no significant difference between the activity of tree no. 2 and that of the other active trees (Fig. 5A), indicating that other compounds can also be responsible of the activity. Two diesterified daphnanes, 20-hexadecanoyl-huratoxin (monoester) and 20-octa-dien-oyl-huratoxin (monoester), show a strong correlation with cytostatic activity on Caco-2 cells (Table 1). However, previous studies have reported that diesterified daphnanes from *H. crepitans* do not exhibit cytostatic activity against these cells [5]. This correlation does not necessarily indicate that these daphnanes are bioactive but suggests that they are more concentrated in the most active extract, which comes from Peruvian tree no. 1 (Figure 6). To explain the superior activity of the latex from tree no. 1 (Fig. 5A), it can be expected that other minor monoesterified daphnanes are exclusively present in this tree's latex and potentiate the effect of huratoxin. This conjecture is supported by the mass spectral similarity network (Fig. 4), where several potential active monoesterified daphnanes are present in the Peruvian *Hura* latexes. It would be interesting to isolate these new compounds, with a particular interest in the monoesterified daphanes from the latex of Peruvian tree no. 1.

3.3.2. Activities against Hela and Jurkat cells

Cytotoxic assays were also conducted on Jurkat and Hela cell lines to identify other potential bioactive compounds besides daphnanes. An extract from each tree was tested, and the mean effect of trees from the same collection site was calculated. As shown in Fig. 7A, which displays the cytotoxic activity of latex extracts from Peruvian and African trees normalized to the effect of DMSO (control), only the samples collected in Ouidah and Ahita exhibit a significant effect, inhibiting Hela cell proliferation by approximately 20–30 %, surpassing the activity of doxorubicin at 1 μg/mL (17 %). A similar result was obtained with the Jurkat cells (Fig. 7B) assay, with a slight effect from the Peruvian samples, resulting in about 10 % proliferation inhibition. Doxorubicin inhibited Jurkat cell growth by approximately 57 % at 1 μg/mL, which is significantly higher than the inhibition observed with our extracts. Surprisingly, Ouidah and Ahita extracts are separated on the PCA and OPLS-DA built according to the phytochemical compositions (Figs. 2A and 2B). Therefore, these activities are most likely due to different compounds in the samples collected in Ouidah and Ahita. This distinction probably contributes to the failure of multivariate analyses to pinpoint specific cytotoxic compounds, necessitating the use of univariate analyses to identify correlations between individual chemical features and growth inhibition on Jurkat and Hela cells.

Ten compounds showed a correlation coefficient greater than 0.6 and were correlated with the inhibition of Hela cell proliferation. The top three are listed in Table 2. The first one was annotated as elasterol (level 3), a steroid, followed by two cerebrosides. To our knowledge, elasterol has not been previously described in *Euphorbia* species. Consequently, it would be interesting to isolate it to confirm this annotation, despite the potential difficulty due to its low abundance. Therefore, this is supported by the fact that numerous steroids have been previously described in *Euphorbia* species [23–26]. In the literature, several biological activities of phytosterol derivatives have been suggested, notably antibacterial and anticancer activities [27–29]. Regarding the cerebrosides, some were incorrectly annotated by the MS Finder software due to their fragmentation (a systematic loss of glucose moiety) in the atmospheric pressure chemical ionization probe leading to a false annotation of the fragment as a molecular ion. These compounds were therefore manually annotated by examining their MS and MSMS spectra. Cerebrosides have already been described in the literature for their biological activities, including anticancer properties [30–32]. However, to our knowledge, they have not been specifically described for their cytotoxicity against Hela cells.

In contrast, the correlation coefficients for compounds correlated with cytotoxic activity against Jurkat cells are below 0.6. Consequently, we were unable to establish any significant correlation between the phytochemical composition of the extracts and this activity. Therefore, in this case, only bioguided fractionation can lead to the identification of the compounds responsible for this activity.

4. Conclusion

This study provides a comprehensive analysis of the phytochemical

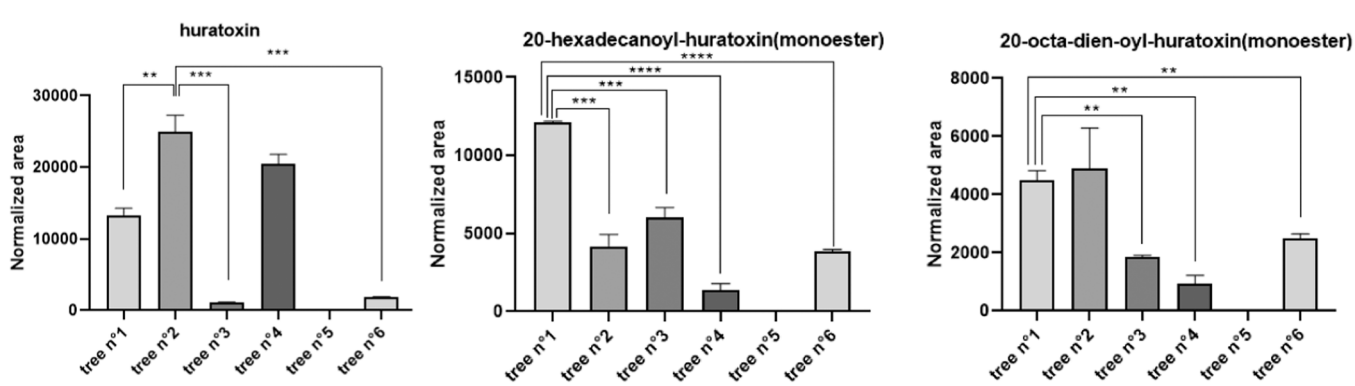

Fig. 6. Normalized peak areas of the top three compounds correlated with potential cytostatic activity on Caco-2 cells for each Peruvian tree. Mean ± SEM, *t*-test from triplicates of extraction. ** $p < 0.01$, *** $p < 0.001$, **** $p < 0.0001$.

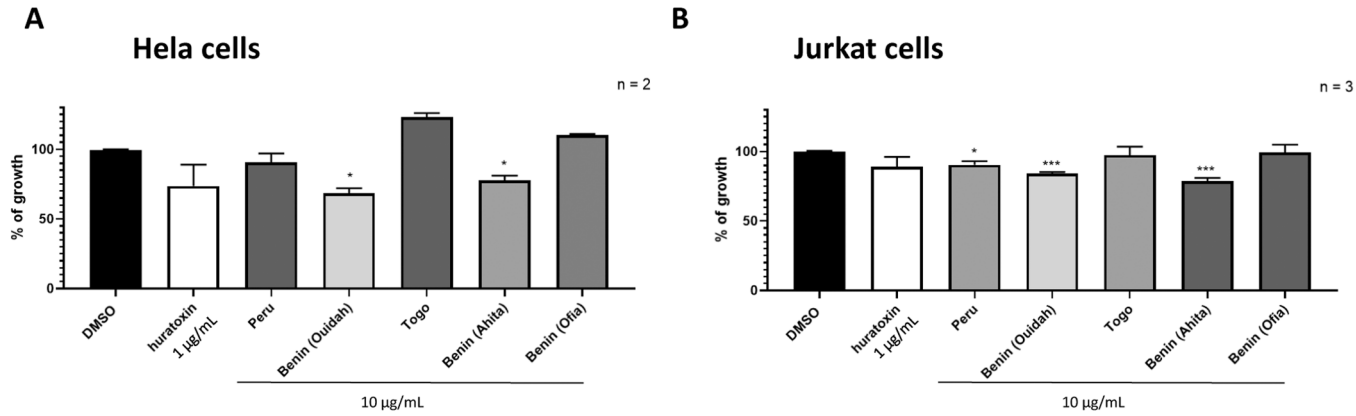

Fig. 7. Cytotoxic activity of *H. crepitans* latex extracts on Hela (A) and Jurkat (B) cells. Cells were incubated with extracts (10 µg/mL) or huratoxin (1 µg/mL) as a positive control during 48 h then cell viability was measured by colorimetry and compared to control (DMSO). Mean ± SEM, *t*-test from triplicates of 2–3 independent experiments. * $p < 0.05$, *** $p < 0.001$.

Table 2
Top three compounds correlated with the cytotoxic activity on Hela cells.

Rank	$[M+H]^+$	RT (min)	MF	Correlation coefficients	*Annotation*
1	**411.36365**	13.93	$C_{29}H_{46}O$	0.73270714	**Steroid** *elasterol*
2	**598.57764** *Fragment of 760.63031*	16.98	$C_{42}H_{81}NO_{10}$	0.68877741	**Cerebroside** *GlcCer(d19:1(6)/17:1(1)(4OH))*
3	**612.59271** *Fragment of 774.64673*	19.46	$C_{44}H_{87}NO_9$	0.67717051	**Cerebroside** *GlcCer(d20:0/18:0(2OH)*

composition and cytotoxic activities of *Hura crepitans* latex extracts from Peru, Benin, and Togo. Metabolomic approaches and multivariate analysis revealed significant differences in the phytochemical profiles of extracts from various collection sites. Intercontinental differences were evident, with daphnane compounds concentrated in Peruvian samples, explaining their cytostatic activity on Caco-2 cells. African samples were categorized into two groups according to their chemical composition: latex collected in Ouidah (Benin) and Togo contained mainly sphingolipids, while latex from Ahita and Ofia (Benin) contained terpenoids (excluding daphnanes) and sphingolipids. Intra-continental differences may be attributed to the developmental stage of the trees. Notably, samples from Ouidah and Ahita exhibited cytostatic activity on Jurkat and Hela cells. Univariate analyses identified significant correlations between specific compounds and the inhibition of Hela cell proliferation, with a steroid annotated as elasterol and two cerebrosides showing the highest correlation. These findings suggest that these compounds may contribute to the observed cytotoxic effects and warrant further investigation to confirm their identities and biological activities. The diverse metabolites in *Hura crepitans* latexes reflect the plant's adaptive responses to varying environmental conditions, offering valuable insights into the chemical ecology and therapeutic potential of this species. As *Hura crepitans* is used in plantations as a pepper tree stake in various sub-Saharan African countries, it generates a latex biomass that could be used to produce complex bioactive molecules.

Funding

This work was supported by the French Ministry of Higher Education and Research.

CRediT authorship contribution statement

Guillaume Marti: Writing – review & editing, Visualization, Validation, Supervision, Methodology, Investigation, Formal analysis, Conceptualization. **Nicolas Fabre:** Writing – review & editing, Supervision, Project administration, Conceptualization. **Mamoudou Alao:** Resources, Conceptualization. **Arthur-Joel Semedo:** Resources. **Hospice Dassou:** Resources. **Pedro Vásquez-Ocmín:** Writing – review & editing, Resources. **Gabriel Vargas-Arana:** Resources. **Elise Crossay:** Writing – original draft, Validation, Methodology, Investigation, Formal analysis, Data curation, Conceptualization. **Valérie Cristofoli:** Methodology.

Declaration of Generative AI and AI-assisted technologies in the writing process

During the preparation of this work, the authors used ChatGPT to enhance the English language of the manuscript. After using this tool/service, the authors carefully reviewed and edited the content as needed and take full responsibility for the content of the published article.

Declaration of Competing Interest

The authors declare that they have no known competing financial interests or personal relationships that could have appeared to influence the work reported in this paper.

Acknowledgements

We would like to thank Nallarett Davila (Instituto de Investigaciones de la Amazonía Peruana (IIAP), Av. Abelardo Quiñonez km 2.5, Iquitos, Peru) for her invaluable assistance in the collection of *Hura crepitans* L. latex in the Amazon rainforest.

Supplementary data

The **StatTable.csv** file contains peak area data and annotations for all features. It was uploaded to Simca.14 software to perform statistical analysis on the dataset.

The **Nodes.csv** and **EdgeAll.csv** files contain all the necessary data and annotations required to construct the molecular network. These files were directly uploaded into Cytoscape software. The Node.csv file likely contains information about individual molecules or features, while the Edge.csv file defines the relationships or connections between these molecules.

Appendix A. Supporting information

Supplementary data associated with this article can be found in the online version at doi:10.1016/j.jpba.2024.116583.

Data Availability

Raw data are available at: 10.5281/zenodo.13753688.

References

[1] O.S. Owojuyigbe, C.K. Firempong, C. Larbie, G. Komlaga, B.O. Emikpe, Hepatoprotective potential of Hura crepitans L.: a review of ethnomedical, phytochemical and pharmacological studies, J. Complement. Altern. Med. Res. 9 (2020) 1–10, https://doi.org:10.9734/jocamr/2020/v9i230136.

[2] A.B. Kadiri, S. Adeniran, Study of the anatomy of the genus Hura L. (Euphorbiaceae), Ife J. Sci. 18 (2016) 413–426.

[3] L. Hura cepitans, Inventaire Natl. Patrim. Nat. 1753 (2003). ⟨https://inpn.mnhn.fr/espece/cd_nom/629870⟩ (accessed July 28, 2022).

[4] M. Trinel, V. Jullian, A.-C. Le Lamer, I. Mhamdi, K. Mejia, D. Castillo, B. J. Cabanillas, N. Fabre, Profiling of *Hura crepitans* L. latex by ultra-high-performance liquid chromatography/atmospheric pressure chemical ionisation linear ion trap Orbitrap mass spectrometry, Phytochem. Anal. 29 (2018) 627–638, https://doi.org/10.1002/pca.2776.

[5] M. Trinel, A.-C. Le Lamer, V. Jullian, D. Jacquemin, J. Graton, V. Cristofoli, E. Crossay, M. Yassine, C. Rolland, N. Vergnolle, K. Mejia, B. Joel Cabanillas, C. Racaud-Sultan, N. Fabre, Daphnanes diterpenes from the latex of Hura crepitans L. and activity against human colorectal cancer cells Caco-2, Bioorg. Chem. 103 (2020) 1–13, https://doi.org/10.1016/j.bioorg.2020.104132.

[6] E. Crossay, V. Jullian, M. Trinel, D. Sagnat, D. Hamel, E. Groppi, C. Rolland, J.-L. Stigliani, K. Mejia, B.J. Cabanillas, L. Alric, E. Buscail, C. El Kalamouni, P. Mavingui, C. Deraison, C. Racaud-Sultan, N. Fabre, Daphnanes diterpenes from the latex of Hura crepitans L. and their PKCζ-dependent anti-proliferative activity on colorectal cancer cells, Bioorg. Med. Chem. 90 (2023) 117366, https://doi.org/10.1016/j.bmc.2023.117366.

[7] Y. Xi, P. Xu, Global colorectal cancer burden in 2020 and projections to 2040, Transl. Oncol. 14 (2021) 1–7, https://doi.org/10.1016/j.tranon.2021.101174.

[8] M.A. Juanes, Cytoskeletal control and Wnt signaling—APC's dual contributions in stem cell division and colorectal cancer, Cancers 12 (2020) 1–21, https://doi.org/10.3390/cancers12123811.

[9] W. Hankey, Functions of the APC tumor suppressor protein dependent and independent of canonical WNT signaling: implications for therapeutic targeting, Cancer Metastas-.-. Rev. 37 (2018) 159–172.

[10] G. Oloyede, O. Adaramoye, M. Olatinwo, Chemical constituents of sandbox tree (Hura crepitans Linn.) and anti-hepatotoxic activity of the leaves and stem bark extracts, West Indian Med. J. (2016) 1–27, https://doi.org/10.7727/wimj.2015.247.

[11] F.C. Akharaiyi, O.O.O. Odiedi, J.A. Johnson, F.S. Oluwafemi, Inhibitory effect and preliminary phytochemical screening of some ornemental plants against some bacteria pathogens, Eurasia J. Biosci. 13 (2019) 899–908.

[12] J.-L. Wolfender, G. Marti, A. Thomas, S. Bertrand, Current approaches and challenges for the metabolite profiling of complex natural extracts, J. Chromatogr. A 1382 (2015) 136–164, https://doi.org/10.1016/j.chroma.2014.10.091.

[13] F. Mehl, G. Marti, J. Boccard, B. Debrus, P. Merle, E. Delort, L. Baroux, V. Raymo, M.I. Velazco, H. Sommer, J.-L. Wolfender, S. Rudaz, Differentiation of lemon essential oil based on volatile and non-volatile fractions with various analytical techniques: a metabolomic approach, Food Chem. 143 (2014) 325–335, https://doi.org/10.1016/j.foodchem.2013.07.125.

[14] H. Tsugawa, T. Cajka, T. Kind, Y. Ma, B. Higgins, K. Ikeda, M. Kanazawa, J. VanderGheynst, O. Fiehn, M. Arita, MS-DIAL: data-independent MS/MS deconvolution for comprehensive metabolome analysis, Nat. Methods 12 (2015) 523–526, https://doi.org/10.1038/nmeth.3393.

[15] O. Fraisier-Vannier, J. Chervin, G. Cabanac, V. Puech, S. Fournier, V. Durand, A. Amiel, O. André, O.A. Benamar, B. Dumas, H. Tsugawa, G. Marti, MS-CleanR: a feature-filtering workflow for untargeted LC–MS based metabolomics, Anal. Chem. 92 (2020) 9971–9981, https://doi.org/10.1021/acs.analchem.0c01594.

[16] H. Tsugawa, T. Kind, R. Nakabayashi, D. Yukihira, W. Tanaka, T. Cajka, K. Saito, O. Fiehn, M. Arita, Hydrogen rearrangement rules: computational MS/MS fragmentation and structure elucidation using MS-FINDER software, Anal. Chem. 88 (2016) 7946–7958, https://doi.org/10.1021/acs.analchem.6b00770.

[17] L.W. Sumner, A. Amberg, D. Barrett, M.H. Beale, R. Beger, C.A. Daykin, T.W.-M. Fan, O. Fiehn, R. Goodacre, J.L. Griffin, T. Hankemeier, N. Hardy, J. Harnly, R. Higashi, J. Kopka, A.N. Lane, J.C. Lindon, P. Marriott, A.W. Nicholls, M.D. Reily, J.J. Thaden, M.R. Viant, Proposed minimum reporting standards for chemical analysis: chemical analysis working group (CAWG) metabolomics standards initiative (MSI), Metabolomics 3 (2007) 211–221, https://doi.org/10.1007/s11306-007-0082-2.

[18] P. Shannon, A. Markiel, O. Ozier, N.S. Baliga, J.T. Wang, D. Ramage, N. Amin, B. Schwikowski, T. Ideker, Cytoscape: a software environment for integrated models of biomolecular interaction networks, Genome Res. 13 (2003) 2498–2504, https://doi.org/10.1101/gr.1239303.

[19] L.F. Salomé-Abarca, D. Gođevac, M.S. Kim, G.-S. Hwang, S.C. Park, Y.P. Jang, C.A. J. Van Den Hondel, R. Verpoorte, P.G.L. Klinkhamer, Y.H. Choi, Latex metabolome of euphorbia species: geographical and inter-species variation and its proposed role in plant defense against herbivores and pathogens, J. Chem. Ecol. 47 (2021) 564–576, https://doi.org/10.1007/s10886-021-01274-x.

[20] P. Rodziewicz, B. Swarcewicz, K. Chmielewska, A. Wojakowska, M. Stobiecki, Influence of abiotic stresses on plant proteome and metabolome changes, Acta Physiol. Plant. 36 (2014) 1–19, https://doi.org/10.1007/s11738-013-1402-y.

[21] H. Zheng, M.-Y. Yu, Y. Han, B. Tai, S.-F. Ni, R.-F. Ji, C.-J. Pu, K. Chen, F.-Q. Li, H. Xiao, Y. Shen, X.-T. Zhou, L.-Q. Huang, Comparative transcriptomics and metabolites analysis of two closely related euphorbia species reveal environmental adaptation mechanism and active ingredients difference, Front. Plant Sci. 13 (2022) 905275, https://doi.org/10.3389/fpls.2022.905275.

[22] W. Adolf, E. Hecker, On the active principles of the spurge family, X. 1,2 skin irritants, cocarcinogens, and cryptic cocarcinogens from the latex of the manchineel Tree, J. Nat. Prod. 47 (1984) 482–496, https://doi.org/10.1021/np50033a015.

[23] M.P. Stracke, B.T.K. Tusset, R. de, F. Franzin, Extraction and characterization of latex from the Euphorbia tirucalli, Int. J. Dev. Res. 11 (2021) 45406–45415.

[24] J.-C. Li, S.-Y. Li, J.-X. Tang, D. Liu, X.-Y. Feng, K.-R. Rao, X.-D. Zhao, H.-M. Li, R.-T. Li, Triterpenoids, steroids and other constituents from Euphorbia kansui and their anti-inflammatory and anti-tumor properties, Phytochemistry 204 (2022) 113449, https://doi.org/10.1016/j.phytochem.2022.113449.

[25] J.-X. Zhao, S.-S. Shi, L. Sheng, J. Li, J.-M. Yue, Terpenoids and steroids from *Euphorbia hypericifolia*, Nat. Prod. Commun. 10 (2015) 2049–2052, https://doi.org/10.1177/1934578X1501001209.

[26] Z. Al-Ansi, M. Masaoud, K. Hussein, B. Moharram, W.M. Al-Madhagi, Antibacterial and antioxidant activities of triterpenoids isolated from endemic euphorbia arbuscula stem latex, Adv. Pharmacol. Pharm. Sci. 2024 (2024) 1–9, https://doi.org/10.1155/2024/8273789.

[27] V.R. Ramprasath, A.B. Awad, Role of phytosterols in cancer prevention and treatment, J. AOAC Int. 98 (2015) 735–738, https://doi.org/10.5740/jaoacint.SGERamprasath.

[28] C. Katariya, S. Malaiappan, Antimicrobial activity of mint extract on periodontopathic bacteria-an in-vitro study, J. Res. Med. Dent. Sci. 10 (2022) 509–520.

[29] A.P. Echavarría, H. D'Armas, N. Matute, A. Cano, Phytochemical analyses of eight plants from two provinces of Ecuador by GC-MS, Int. J. Herb. Med. 8 (2020) 10–20.

[30] G.R. Ebede, J.T. Ndongo, J.N. Mbing, H.C.M. Kenfack, D.E. Pegnyemb, C. G. Bochet, Contortamide, a new anti-colon cancer cerebroside and other constituents from *Tabernaemontana contorta* Stapf (Apocynaceae), Nat. Prod. Res. 35 (2021) 1757–1765, https://doi.org/10.1080/14786419.2019.1636243.

[31] S.R. Lee, K. Jung, H.J. Noh, Y.J. Park, H.L. Lee, K.R. Lee, K.S. Kang, K.H. Kim, A new cerebroside from the fruiting bodies of Hericium erinaceus and its applicability to cancer treatment, Bioorg. Med. Chem. Lett. 25 (2015) 5712–5715, https://doi.org/10.1016/j.bmcl.2015.10.092.

[32] P.G. De Souza, A. Rosenthal, E.M.M. Ayres, A.J. Teodoro, Potential functional food products and molecular mechanisms of portulaca oleracea L. on anticancer activity: a review, Oxid. Med. Cell. Longev. 2022 (2022) 1–9, https://doi.org/10.1155/2022/7235412.